International Journal of Engineering and Technologies
ISSN: 2297-623X, Vol. 7, pp 1-24
doi:10.18052/www.scipress.com/IJET.7.1
CC BY 4.0. Published by SciPress Ltd, Switzerland, 2016

Submitted: 2016-02-09
Accepted: 2016-03-22
Online: 2016-05-16

Performance Evaluation of Free Vibration of Laminated Composite Stiffened Hyperbolic Paraboloid Shell Panel with Cutout

Sarmila Sahoo

Department of Civil Engineering, Heritage Institute of Technology, Kolkata 700107, India

E-mail: sarmila.sahoo@gmail.com, sarmila_ju@yahoo.com

Keywords: laminated composites; hyperbolic paraboloid shell panel; cutout; stiffener; free vibration; finite element.

Abstract. The paper considers free vibration characteristics of stiffened composite hyperbolic paraboloid shell panel with cutout in terms of natural frequency and mode shapes. A finite element code is developed for the purpose by combining an eight noded curved shell element with a three noded curved beam element. The size of the cutouts and their positions with respect to the shell centre are varied for different edge conditions of cross-ply and angle-ply laminated shells. The effects of these parametric variations on the fundamental frequencies and mode shapes are considered in details to conclude a set of inferences of practical engineering significance.

Notations

a ,b	length and width of shell in plan
$a^{/}$,$b^{/}$	length and width of cutout in plan
b_{st}	width of stiffener in general
b_{sx}, b_{sy}	width of x and y stiffeners respectively
B_{sx}, B_{sy}	strain displacement matrix of stiffener elements
d_{st}	depth of stiffener in general
d_{sx}, d_{sy}	depth of x and y stiffeners respectively
$\{d_e\}$	element displacement
e_{sx}, e_{sy}	eccentricities of x and y -stiffeners with respect to shell mid-surface respectively
E_{11}, E_{22}	elastic moduli
G_{12}, G_{13}, G_{23}	shear moduli of a lamina with respect to 1, 2 and 3 axes of fibre
h	shell thickness
M_x, M_y	moment resultants
M_{xy}	torsion resultant
np	number of plies in a laminate
N_1-N_8	shape functions
N_x, N_y	inplane force resultants
N_{xy}	inplane shear resultant
Q_x, Q_y	transverse shear resultant
R_{xx}, R_{yy}, R_{xy}	radii of curvature and cross curvature of shell respectively
u, v, w	translational degrees of freedom
x, y, z	local co-ordinate axes
X, Y, Z	global co-ordinate axes
z_k	distance of bottom of the kth ply from mid-surface of a laminate
α,β	rotational degrees of freedom
ε_x, ε_y	inplane strain component
γ_{xy} ,γ_{xz}, γ_{yz}	shearing strain components
ν_{12}, ν_{21}	Poisson's ratios
ξ, η, τ	isoparametric co-ordinates
ρ	density of material

σ_x, σ_y	inplane stress components
τ_{xy}, τ_{xz}, τ_{yz}	shearing stress components
ω	natural frequency
$\bar{\omega}$	non-dimensional natural frequency $= \omega a^2 \left(\rho / E_{22} h^2\right)^{1/2}$

Introduction

Composite shell structures are extensively used in aerospace, civil, marine and other engineering applications. In practical civil engineering applications, the necessity of covering large column free open areas is often an issue. It is advantageous to use thin shells instead of flat plates to cover large column free open spaces as in airports, parking lots, hangers, and the like. Such areas in medical plants and automobile industries prefer entry of north light through the roofing units. Quite often, to save weight and also to provide a facility for inspection, cutouts are provided in shell panels. In practice the margin of the cutouts must be stiffened to take account of stress concentration effects. In civil engineering construction, conoidal hyperbolic paraboloid (among the anticlastic) and elliptic paraboloid (among the synclastic) shells are used as roofing units to cover large column free areas. The hyperbolic paraboloid shells are aesthetically appealing although they offer less stiffness than other doubly curved shells. Now-a-days, civil engineers use laminated composites to fabricate these shell forms as the high specific stiffness and strength properties of these materials result in less gravity forces and mass-induced forces (seismic force) on the laminated shells compared to their isotropic counterparts. All these taken together reduce the foundation costs to a great extent. Realizing the importance of laminated composite doubly curved shells in the industry, several aspects of shell behaviour such as bending, buckling, vibration, impact etc. are being reported by different researchers. The present investigation is however, restricted only to the free vibration behaviour of composite stiffened hyperbolic paraboloid shell panels with cutout.

No wonder a number of researchers are working to explore different behavioral aspects of laminated doubly curved shells. Researchers like Ghosh and Bandyopadhyay [1], Dey et al. [2, 3], Chakravorty et al. [4, 5] reported static and dynamic behaviour of laminated doubly curved shells. Later Nayak and Bandyopadhyay [6-8], Das and Chakravorty [9-12] and Pradyumna and Bandyopadhyay [13, 14] reported static, dynamic and instability behaviour of laminated doubly curved shells. Application of doubly curved shells in structures often necessitates provision of cutouts for the passage of light, service lines and also sometimes for alteration of the resonant frequency. The free vibration of composite as well as isotropic plate with cutout was studied by different researchers from time to time. Reddy [15] investigated large amplitude flexural vibration of composite plate with cutout. Malhotra et al. [16] studied free vibration of composite plate with cutout for different boundary conditions. One of the early reports on free vibration of curved panels with cutout was due to Sivasubramonian et al. [17]. They analysed the effect of cutouts on the natural frequencies of plates with some classical boundary conditions. The plate had a curvature in one direction and was straight in the other. The effect of fibre orientation and size of cutout on natural frequency on orthotropic square plates with square cutout was studied using Rayleigh-Ritz method. Later Sivakumar et al. [18], Rossi [19], Huang and Sakiyama [20] and Hota and Padhi [21] studied free vibration of plate with various cutout geometries. Chakravorty et al. [22] analysed the effect of concentric cutout on different shell options. Sivasubramonian et al. [23] studied the effect of curvature and cutouts on square panels with different boundary conditions. The size of the cutout (symmetrically located) as well as curvature of the panels is varied. Hota and Chakravorty [24] published useful information about free vibration of stiffened conoidal shell roofs with cutout. Later Nanda and Bandyopadhyay [25], Kumar et al. [26] studied the effect of different parametric variation on free vibration of cylindrical shell with cutout using first order shear deformation theory (FSDT) and higher order shear deformation theory (HYSD) respectively.

It is noted from the literature review that free vibration study of laminated composite hyperbolic paraboloid shell panels with cutout is not reported by any researcher so far although the importance of this shell form is mentioned. Thus the present study intends to study the free vibration behaviour of stiffened hyperbolic paraboloid shell panels with cutout by varying the size and position of the cutouts.

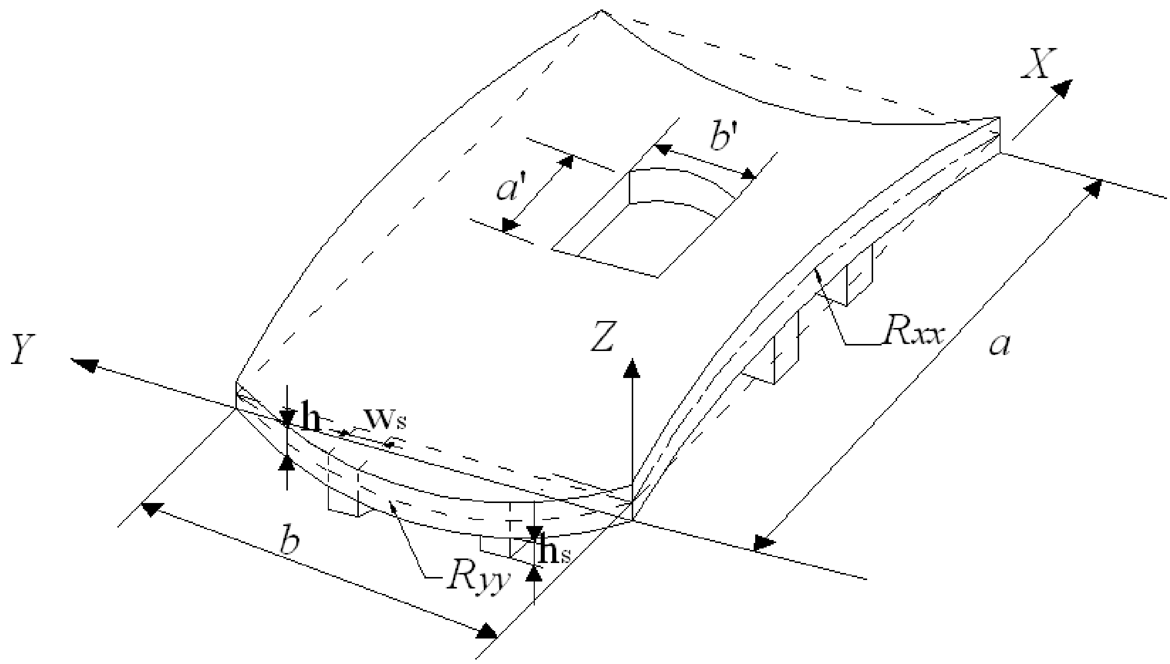

Fig.1 Hyperbolic paraboloid shell with a concentric cutout stiffened along the margins

Mathematical formulation

A laminated composite hyperbolic paraboloid shell of uniform thickness h (Fig.1) and radius of curvature R_{xx} and R_{yy} is considered. Keeping the total thickness the same, the thickness may consist of any number of thin laminae each of which may be arbitrarily oriented at an angle θ with reference to the x-axis of the co-ordinate system. The constitutive equations for the shell are given by (a list of notations is already given):

$$\{F\}=[E]\{\varepsilon\} \tag{1}$$

where, $\{F\}=\{N_x, \; N_y, \; N_{xy}, \; M_x, \; M_y, \; M_{xy}, \; Q_x, \; Q_y\}^T$,

$$[E]=\begin{bmatrix}[A] & [B] & [0]\\ [B] & [D] & [0]\\ [0] & [0] & [S]\end{bmatrix}, \; \{\varepsilon\}=\{\varepsilon_x^0, \; \varepsilon_y^0, \; \gamma_{xy}^0, \; k_x, \; k_y, \; k_{xy}, \; \gamma_{xz}^0, \; \gamma_{yz}^0\}^T.$$

The force and moment resultants are expressed as

$$\{N_x, \; N_y, \; N_{xy}, \; M_x, \; M_y, \; M_{xy}, \; Q_x, \; Q_y\}^T = \int_{-h/2}^{h/2}\{\sigma_x, \; \sigma_y, \; \tau_{xy}, \; \sigma_z.z, \; \sigma_y.z, \; \tau_{xy}.z, \; \tau_{xz}, \; \tau_{yz}\}^T dz \tag{2}$$

The submatrices [A], [B], [D] and [S] of the elasticity matrix [E] are functions of Young's moduli, shear moduli and the Poisson's ratio of the laminates. They also depend on the angle which the individual lamina of a laminate makes with the global x-axis. The detailed expressions of the elements of the elasticity matrix are available in several references including Vasiliev et al. [27] and Qatu [28].

The strain-displacement relations on the basis of improved first order approximation theory for thin shell [2] are established as

$$\{\varepsilon_x, \ \varepsilon_y, \ \gamma_{xy}, \ \gamma_{xz}, \ \gamma_{yz}\}^T = \{\varepsilon_x^0, \ \varepsilon_y^0, \ \gamma_{xy}^0, \ \gamma_{xz}^0, \ \gamma_{yz}^0\}^T + z\{k_x, \ k_y, \ k_{xy}, \ k_{xz}, \ k_{yz}\}^T \quad (3)$$

where, the first vector is the mid-surface strain for a hyperbolic paraboloid shell and the second vector is the curvature.

Formulation for Shell

An eight-noded curved quadratic isoparametric finite element is used for shell analysis. The five degrees of freedom taken into consideration at each node are u, v, w, α, β. The following expressions establish the relations between the displacement at any point with respect to the co-ordinates ξ and η and the nodal degrees of freedom.

$$u = \sum_{i=1}^{8} N_i u_i \quad v = \sum_{i=1}^{8} N_i v_i \quad w = \sum_{i=1}^{8} N_i w_i \quad \alpha = \sum_{i=1}^{8} N_i \alpha_i \quad \beta = \sum_{i=1}^{8} N_i \beta_i \quad (4)$$

where the shape functions derived from a cubic interpolation polynomial are:

$N_i = (1+\xi\xi_i)(1+\eta\eta_i)(\xi\xi_i+\eta\eta_i-1)/4$, for i=1,2,3,4
$N_i = (1+\xi\xi_i)(1-\eta^2)/2$, for i=5,7
$Ni = (1+\eta\eta_i)(1-\xi^2)/2$, for i=6,8 (5)

The generalized displacement vector of an element is expressed in terms of the shape functions and nodal degrees of freedom as:

$$[u] = [N]\{d_e\} \quad (6)$$

$$\text{i.e., } \{u\} = \begin{Bmatrix} u \\ v \\ w \\ \alpha \\ \beta \end{Bmatrix} = \sum_{i=1}^{8} \begin{bmatrix} N_i & & & & \\ & N_i & & & \\ & & N_i & & \\ & & & N_i & \\ & & & & N_i \end{bmatrix} \begin{Bmatrix} u_i \\ v_i \\ w_i \\ \alpha_i \\ \beta_i \end{Bmatrix}$$

Element Stiffness Matrix

The strain-displacement relation is given by $\{\varepsilon\} = [B]\{d_e\}$, (7)

$$\text{where } [B] = \sum_{i=1}^{8} \begin{bmatrix} N_{i,x} & 0 & -\frac{N_i}{R_{xx}} & 0 & 0 \\ 0 & N_{i,y} & -\frac{N_i}{R_{yy}} & 0 & 0 \\ N_{i,y} & N_{i,x} & -2N_i/R_{xy} & 0 & 0 \\ 0 & 0 & 0 & N_{i,x} & 0 \\ 0 & 0 & 0 & 0 & N_{i,y} \\ 0 & 0 & 0 & N_{i,y} & N_{i,x} \\ 0 & 0 & N_{i,x} & N_i & 0 \\ 0 & 0 & N_{i,y} & 0 & N_i \end{bmatrix} \quad (8)$$

The element stiffness matrix is

$$[K_e] = \iint [B]^T [E][B] dxdy \quad (9)$$

Element Mass Matrix

The element mass matrix is obtained from the integral

$$[M_e] = \iint [N]^T [P][N] dxdy, \tag{10}$$

where, $[N] = \sum_{i=1}^{8} \begin{bmatrix} N_i & 0 & 0 & 0 & 0 \\ 0 & N_i & 0 & 0 & 0 \\ 0 & 0 & N_i & 0 & 0 \\ 0 & 0 & 0 & N_i & 0 \\ 0 & 0 & 0 & 0 & N_i \end{bmatrix}$, $[P] = \sum_{i=1}^{8} \begin{bmatrix} P & 0 & 0 & 0 & 0 \\ 0 & P & 0 & 0 & 0 \\ 0 & 0 & P & 0 & 0 \\ 0 & 0 & 0 & I & 0 \\ 0 & 0 & 0 & 0 & I \end{bmatrix}$,

in which $P = \sum_{k=1}^{np} \int_{z_{k-1}}^{z_k} \rho dz$ and $I = \sum_{k=1}^{np} \int_{z_{k-1}}^{z_k} z^2 \rho dz$ (11)

Formulation for Stiffener

Three noded curved isoparametric beam elements are used to model the stiffeners, which are taken to run only along the boundaries of the shell elements. In the stiffener element, each node has four degrees of freedom i.e. u_{sx}, w_{sx}, α_{sx} and β_{sx} for x-stiffener and v_{sy}, w_{sy}, α_{sy} and β_{sy} for y-stiffener. The generalized force-displacement relation of stiffeners can be expressed as:

x-stiffener: $\{F_{sx}\} = [D_{sx}]\{\varepsilon_{sx}\} = [D_{sx}][B_{sx}]\{\delta_{sxi}\}$;

y-stiffener: $\{F_{sy}\} = [D_{sy}]\{\varepsilon_{sy}\} = [D_{sy}][B_{sy}]\{\delta_{syi}\}$ (12)

where, $\{F_{sx}\} = [N_{sxx} \quad M_{sxx} \quad T_{sxx} \quad Q_{sxxz}]^T$; $\{\varepsilon_{sx}\} = [u_{sx.x} \quad \alpha_{sx.x} \quad \beta_{sx.x} \quad (\alpha_{sx} + w_{sx.x})]^T$

and $\{F_{sy}\} = [N_{syy} \quad M_{syy} \quad T_{syy} \quad Q_{syyz}]^T$; $\{\varepsilon_{sy}\} = [v_{sy.y} \quad \beta_{sy.y} \quad \alpha_{sy.y} \quad (\beta_{sy} + w_{sy.y})]^T$

The generalized displacements of the x-stiffener and the shell are related by the transformation matrix $\{\delta_{sxi}\} = [T_x]\{\delta\}$ where

$$[T_x] = \begin{bmatrix} 1 + \frac{e_{sx}}{R_{xx}} & symmetric & & \\ 0 & 1 & & \\ 0 & 0 & 1 & \\ 0 & 0 & 0 & 1 \end{bmatrix} \tag{13}$$

The generalized displacements of the y-stiffener and the shell are related by the transformation matrix $\{\delta_{syi}\} = [T_y]\{\delta\}$ where

$$[T_y] = \begin{bmatrix} 1 + \frac{e_{sy}}{R_{yy}} & symmetric & & \\ 0 & 1 & & \\ 0 & 0 & 1 & \\ 0 & 0 & 0 & 1 \end{bmatrix} \tag{14}$$

These transformations are required due to curvature of x-stiffener and y-stiffener. In the above equations, e_{sx} and e_{sy} are the eccentricities of the x-stiffener and y-stiffener. $\{\delta\}$ is the appropriate portion of the displacement vector of the shell.

Elasticity matrices are as follows:

$$[D_{sx}]=\begin{bmatrix} A_{11}b_{sx} & B'_{11}b_{sx} & B'_{12}b_{sx} & 0 \\ B'_{11}b_{sx} & D'_{11}b_{sx} & D'_{12}b_{sx} & 0 \\ B'_{12}b_{sx} & D'_{12}b_{sx} & \frac{1}{6}(Q_{44}+Q_{66})d_{sx}b^3_{sx} & 0 \\ 0 & 0 & 0 & b_{sx}S_{11} \end{bmatrix}$$

$$[D_{sy}]=\begin{bmatrix} A_{22}b_{sy} & B'_{22}b_{sy} & B'_{12}b_{sy} & 0 \\ B'_{22}b_{sy} & \frac{1}{6}(Q_{44}+Q_{66})b_{sy} & D'_{12}b_{sy} & 0 \\ B'_{12}b_{sy} & D'_{12}b_{sy} & D'_{11}d_{sy}b^3_{sy} & 0 \\ 0 & 0 & 0 & b_{sy}S_{22} \end{bmatrix}.$$

where, $D'_{ij} = D_{ij} + 2eB_{ij} + e^2 A_{ij}$; $B'_{ij} = B_{ij} + eA_{ij}$, (15)

and A_{ij}, B_{ij}, D_{ij} and S_{ij} are as explained elsewhere [29].

Here the shear correction factor is taken as 5/6 for the stiffeners. The sectional parameters are calculated with respect to the mid-surface of the shell by which the effect of eccentricities of stiffeners is automatically included. The element stiffness matrices are of the following forms.

for x-stiffener: $[K_{xe}] = \int [B_{sx}]^T [D_{sx}][B_{sx}]dx$;
for y-stiffener: $[K_{ye}] = \int [B_{sy}]^T [D_{sy}][B_{sy}]dy$ (16)

The integrals are converted to isoparametric coordinates and are carried out by 2-point Gauss quadrature. Finally, the element stiffness matrix of the stiffened shell is obtained by appropriate matching of the nodes of the stiffener and shell elements through the connectivity matrix and is given as:

$$[K_e] = [K_{she}] + [K_{xe}] + [K_{ye}]. \quad (17)$$

The element stiffness matrices are assembled to get the global matrices.
Element mass matrix for stiffener element

$[M_{sx}] = \int [N]^T [P][N]dx$ *for x- stiffener*

and $[M_{sy}] = \int [N]^T [P][N]dy$ *for y- stiffener* (18)

Here, $[N]$ is a 3x3 diagonal matrix.

$$[P]=\sum_{i=1}^{3}\begin{bmatrix} \rho.b_{sx}d_{sx} & 0 & 0 & 0 \\ 0 & \rho.b_{sx}d_{sx} & 0 & 0 \\ 0 & 0 & \rho.b_{sx}d^2_{sx}/12 & 0 \\ 0 & 0 & 0 & \rho(b_{sx}.d^3_{sx}+b^3_{sx}.d_{sx})/12 \end{bmatrix} \text{ for x-stiffener}$$

$$[P]=\sum_{i=1}^{3}\begin{bmatrix} \rho.b_{sy}d_{sy} & 0 & 0 & 0 \\ 0 & \rho.b_{sy}d_{sy} & 0 & 0 \\ 0 & 0 & \rho.b_{sy}d^2_{sy}/12 & 0 \\ 0 & 0 & 0 & \rho(b_{sy}.d^3_{sy}+b^3_{sy}.d_{sy})/12 \end{bmatrix} \text{ for y-stiffener}$$

The mass matrix of the stiffened shell element is the sum of the matrices of the shell and the stiffeners matched at the appropriate nodes.

$[M_e] = [M_{she}] + [M_{xe}] + [M_{ye}]$. (19)

The element mass matrices are assembled to get the global matrices.

Cutout consideration

The code developed can take the position and size of cutout as input. The program is capable of generating non uniform finite element mesh all over the shell surface. So the element size is gradually decreased near the cutout margins. Such finite element mesh is redefined in steps and a particular grid is chosen to obtain the fundamental frequency when the result does not improve by more than one percent on further refining. Convergence of results is ensured in all the problems taken up here.

Solution Procedure

The free vibration analysis involves determination of natural frequencies from the condition

$$\left|[K]-\omega^2[M]\right|=0 \tag{20}$$

This is a generalized eigen value problem and is solved by the subspace iteration algorithm.

Results and discussion

First the validation study of the proposed finite element shell model in presence of cutout is carried out. The results of Table 1 show that the agreement of present results with the earlier ones is excellent and the correctness of the stiffener formulation is established. Free vibration of corner point supported, simply supported and clamped spherical shells of $(0/90)_4$ lamination with cutouts is also considered. The fundamental frequencies of spherical shell with cutout obtained by the present method agree well with those reported by Chakravorty et al. [22] as evident from Table 2, establishing the correctness of the cutout formulation in doubly curved shells. Thus it is evident that the finite element model proposed here can successfully analyze vibration problems of stiffened composite hyperbolic paraboloid shell panels with cutout which is reflected by close agreement of present results with benchmark ones.

Table 1: Natural frequency (*Hz*) of centrally stiffened clamped square plate

Mode no.	Mukherjee and Mukhopadhyay [31]	Nayak and Bandyopadhyay [32]		Present method
		N8 (FEM)	N9 (FEM)	
1	711.8	725.2	725.1	733

a=b=0.2032 m, shell thickness =0.0013716 m, stiffener depth 0.0127 m, stiffener width=0.00635 m, stiffener eccentric at bottom, Material property: E=6.87x10^{10} N/m^2, ν=0.29, ρ=2823 kg/m^3

Table 2: Non-dimensional Fundamental Frequencies ($\bar{\omega}$) for laminated composite spherical shell with cutout

a'/a	CS		SS		CL	
	Chakravorty et. al.[22]	Present model	Chakravorty et. al.[22]	Present model	Chakravorty et. al.[22]	Present model
0.0	34.948	34.601	47.109	47.100	118.197	117.621
0.1	35.175	35.926	47.524	47.114	104.274	104.251
0.2	36.528	36.758	48.823	48.801	98.299	97.488
0.3	37.659	37.206	50.925	50.920	113.766	113.226
0.4	39.114	39.412	53.789	53.788	110.601	110.094

a/b=1, a/h=100, a'/b'=1, h/R_{xx}= h/R_{yy}=1/300, CS=Corner point supported, SS=Simply supported, CL=Clamped

In order to study the effect of cutout size and position on the free vibration response additional problems for hyperbolic paraboloid shell panels with 0/90/0/90 and +45/-45/+45/-45 lamination and different boundary conditions have been solved. The positions of the cutouts are varied along both of the plan directions of the shell for different practical boundary conditions to study the effect of eccentricity of cutout on the fundamental frequency.

Behavior of shell panel with concentric cutout

Tables 3 and 4 furnish the results of non-dimensional frequency ($\bar{\omega}$) of 0/90/0/90 and +45/-45/+45/-45 stiffened hyperbolic paraboloid shells with cutout. The shells considered are of square plan form (*a*=*b*) and the cutouts are also taken to be square in plan ($a'=b'$). The cutouts placed concentrically on the shell surface. The cutout sizes (i.e. a'/a) are varied from 0 to 0.4 and boundary conditions are varied along the four edges. The stiffeners are place along the cutout periphery and extended up to the edge of the shell. The boundary conditions are designated by describing the support clamped or simply supported as C or S taken in an anticlockwise order from the edge x=0. This means a shell with CSCS boundary is clamped along *x*=0, simply supported along y=0 and clamped along *x*=*a* and simply supported along *y*=*b*.

Effect of cutout size on fundamental frequency

From Tables 3 and 4 it is seen that when a cutout is introduced to a stiffened shell the fundamental frequency increases in all the cases. This increasing trend is noticed for both cross ply and angle ply shells. This initial increase in frequency is due to the fact that with the introduction of cutout, numbers of stiffeners are increase from two to four in the present study. It is evident from Tables 3 and 4 that in all the cases with the introduction of cutout with a'/a=0.3 the frequencies increase. But further increase in cutout size, fundamental frequencies decrease in few cases. When the cutout size is further increased, but the number and dimensions of the stiffeners do not change, the shell surface undergoes loss of both mass and stiffness as a result fundamental frequency may increase or decrease. As with the introduction of a cutout of a'/a=0.3, in shell surface, the frequency increases in all the cases, this leads to the engineering conclusion that concentric cutouts with stiffened margins may be provided safely on shell surfaces for functional requirements upto a'/a=0.3.

Table 3: Non-dimensional fundamental frequencies ($\bar{\omega}$) for laminated composite (0/90/0/90) stiffened hyperbolic paraboloid shell for different sizes of the central square cutout and different boundary conditions

Boundary conditions	Cutout size (a'/a)				
	0	0.1	0.2	0.3	0.4
CCCC	103.94	118.21	142.85	155.42	157.23
CSCC	82.21	97.37	117.73	133.23	129.29
CCSC	84.52	96.86	115.87	133.89	137.92
CCCS	81.95	96.1	117.23	132.71	129.06
CSSC	66.1	77.91	94.04	109.39	109.2
CCSS	66.04	77.73	94.02	109.38	109.17
CSCS	92.07	91.93	114.27	130.15	127.7
SCSC	90.59	93.61	114.08	131.02	132.55
CSSS	61.19	73.11	90.99	104.18	104.03
SSSC	62.26	74.04	94.4	103.78	102.22
SSCS	61.19	73.18	90.99	104.18	104.03
SSSS	66.21	68.82	88.25	97.8	96.83
Point supported	28.56	33.64	40.85	49.17	57.67

a/*b*=1, *a*/*h*=100, a'/b'=1, *c*/*a*=0.2; $E_{11}/E_{22}=25$, $G_{23}=0.2E_{22}$, $G_{13}=G_{12}=0.5E_{22}$, $\nu_{12}=\nu_{21}=0.25$.

Effect of boundary conditions

The boundary conditions may be arranged in the following order, considering number of boundary constraints: CCCC, CSCC, CCSC, CCCS, CSSC, CCSS, CSCS, SCSC, CSSS, SSSC, SSCS, SSSS and Corner Point supported. Tables 5 and 6 show the efficiency of a particular clamping option in improving the fundamental frequency of a shell panel with minimum number of boundary constraints relative to that of a clamped shell. Marks are assigned to each boundary combination in a scale assigning a value of 0 to the frequency of a corner point supported shell and 100 to that of a fully clamped shell. These marks are furnished for cutouts with a'/a=0.2 These tables will enable a practicing engineer to realize at a glance the efficiency of a particular boundary condition in improving the frequency of a shell, taking that of clamped shell as the upper limit.

Table 4: Non-dimensional fundamental frequencies ($\overline{\omega}$) for laminated composite (+45/-45/+45/-45) stiffened hyperbolic paraboloid shell for different sizes of the central square cutout and different boundary conditions

Boundary conditions	Cutout size (a'/a)				
	0	0.1	0.2	0.3	0.4
CCCC	101.36	119.09	123.64	126.15	129.41
CSCC	91.93	108.2	114.13	115.26	113.36
CCSC	94.41	108.5	113.84	116.84	119.99
CCCS	91.7	107.51	113.95	115.13	113.35
CSSC	84.44	96.76	105.31	108.66	108.55
CCSS	83.77	96.27	105.06	108.64	108.7
CSCS	90.06	105.92	111.18	112.05	110.86
SCSC	92.44	106.55	111.01	113.69	116.84
CSSS	82.22	93.92	102.95	105.28	105.35
SSSC	81.12	95.43	102.26	105.14	105.35
SSCS	82.35	94.2	102.95	105.28	105.35
SSSS	73.24	90.05	96.76	99.26	99.61
Point supported	36.17	42.04	49.86	59.38	61.29

a/b=1, a/h=100, a'/b'=1, c/a=0.2; E_{11}/E_{22} = 25, G_{23} = 0.2E_{22}, G_{13} = G_{12} = 0.5E_{22}, $\nu_{12} = \nu_{21}$ =0.25.

Table 5: Clamping options for 0/90/0/90 hyperbolic paraboloid shells with central cutouts having a'/a ratio 0.2.

Number of sides to be clamped	Clamped edges	Improvement of frequencies with respect to point supported shells	Marks indicating the efficiencies of no of restraints
0	Corner Point supported	-	0
0	Simply supported no edges clamped (SSSS)	Good improvement	46
1	a) hyperbolic edge along x=a (SSCS)	Good improvement	49
	b)hyperbolic edge along x=0 (CSSS)	Good improvement	49
	b) One parabolic edge along y= b (SSSC)	Good improvement	53
2	a)Two hyperbolic edges x=0 and x=a (CSCS)	Marked improvement	72
	b)Two parabolic edges along y=0 and y=b(SCSC)	Marked improvement	72

	c)Any two edges except the above option (CSSC,CCSS)	Good improvement	52
3	3 edges including the two hyperbolic edges (CSCC,CCCS)	Marked improvement	75
	3 edges excluding the hyperbolic edge along x=a (CCSC)	Marked improvement	74
4	All sides (CCCC)	Frequency attains highest value	100

Table 6: Clamping options for +45/-45/+45/-45 hyperbolic paraboloid shells with central cutouts having a'/a ratio 0.2.

Number of sides to be clamped	Clamped edges	Improvement of frequencies with respect to point supported shells	Marks indicating the efficiencies of no of restraints
0	Corner Point supported	-	0
0	Simply supported no edges clamped (SSSS)	Marked improvement	64
1	a) hyperbolic edge along x=a (SSCS)	Marked improvement	72
	b)hyperbolic edge along x=0 (CSSS)	Marked improvement	72
	b) One parabolic edge along y= b (SSSC)	Marked improvement	71
2	a)Two hyperbolic edges x=0 and x=a (CSCS)	Remarkable improvement	83
	b)Two parabolic edges along y=0 and y=b(SCSC)	Remarkable improvement	83
	c)Any two edges except the above option (CSSC,CCSS)	Marked improvement	75
3	3 edges including the two hyperbolic edges (CSCC,CCCS)	Remarkable improvement	87
	3 edges excluding the hyperbolic edge along x=a (CCSC)	Remarkable improvement	87
4	All sides (CCCC)	Frequency attains highest value	100

It is seen from Table 5 and 6, that fundamental frequencies of members belonging to same number of boundary constraints may not have close values for all the cases considered here. So the boundary constraint is not the sole criteria for its performance. The free vibration characteristics mostly depends on the arrangement of boundary constrains rather than their actual number, is evident from the present study. It can be seen from the present study that if the hyperbolic edge along x=a is released from clamped to simply supported, the change of frequency is more in case of a cross ply shells than that for an angle ply shells. Again, if the two adjacent edges are released, fundamental frequency decreases more significantly than that of a shell in which two alternate edges are released. This is true for both cross and angle ply shells. For cross ply shells if three or four edges are simply supported, frequency values undergo marked decrease but for angle ply shells with the introduction of more number of simply supported edges the frequency value does not change so drastically. The results indicate that two alternate edges should preferably be clamped in order to achieve higher frequency values.

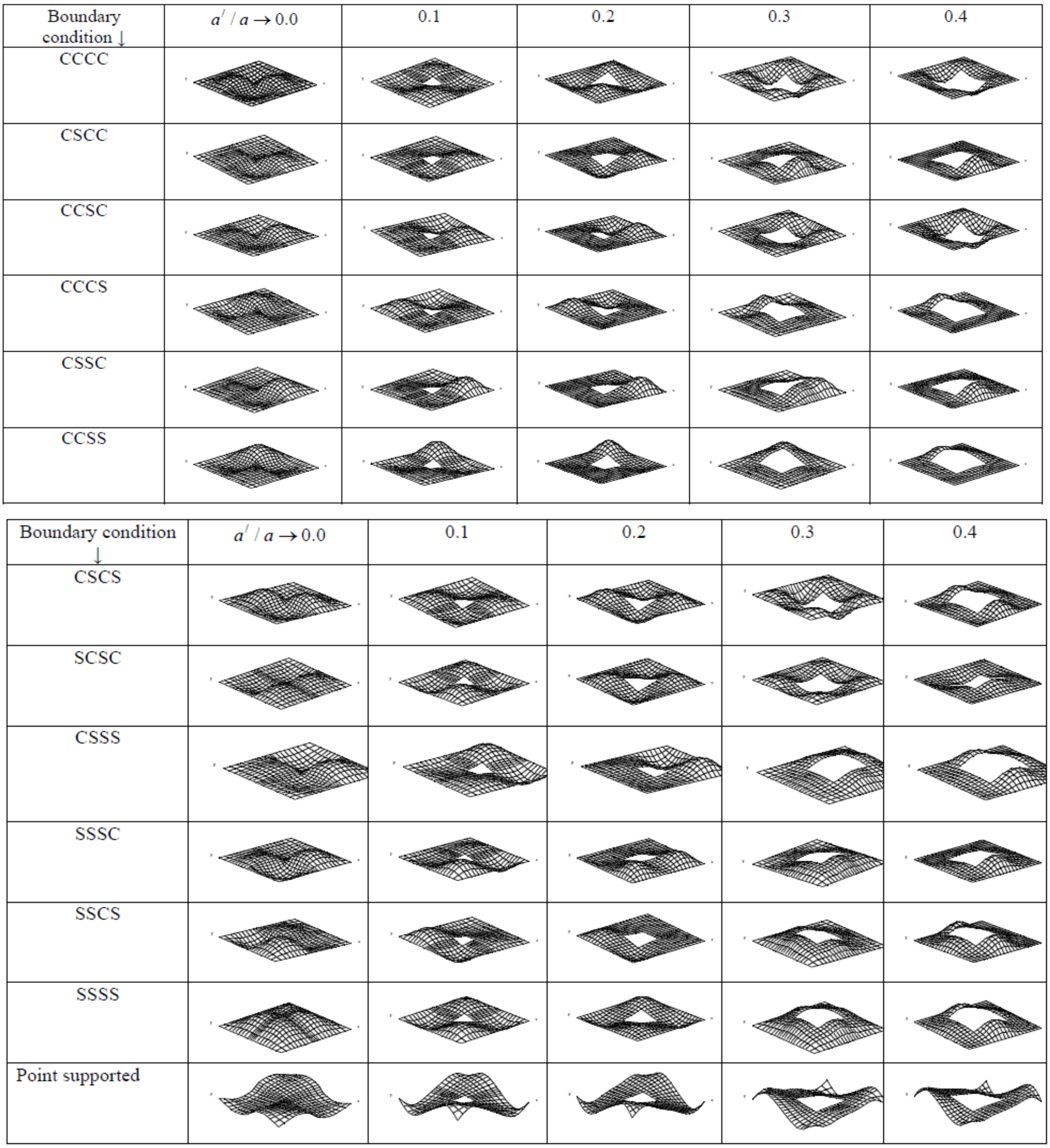

Fig.2: First mode shapes of laminated composite (0/90/0/90) stiffened hyperbolic paraboloid shell for different sizes of the central square cutout and boundary conditions.

Mode shapes

The mode shapes corresponding to the fundamental modes of vibration are plotted in Fig.2 and Fig.3 for cross-ply and angle ply shells respectively. The normalized displacements are drawn with the shell mid-surface as the reference for all the support condition and for all the lamination used here. The fundamental mode is clearly a bending mode or torsion mode for all the boundary condition for cross ply and angle ply shells, except corner point supported shell. For corner point supported shells the fundamental mode shapes are complicated. With the introduction of cutout mode shapes remain almost similar. When the size of the cutout is increased from 0.2 to 0.4 the fundamental modes of vibration do not change to an appreciable amount.

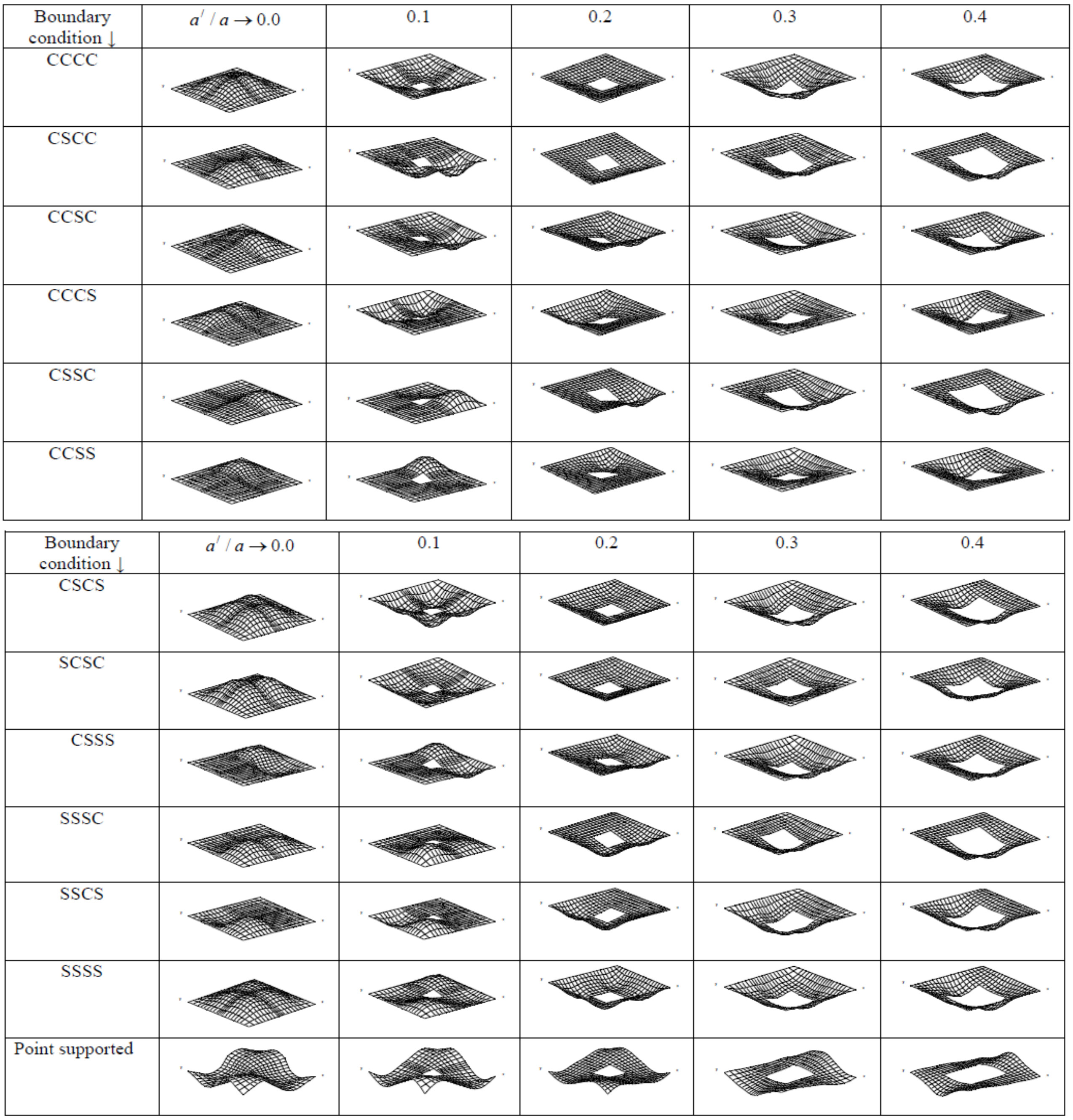

Fig.3: First mode shapes of laminated composite (+45/-45/+45/-45) stiffened hyperbolic paraboloid shell for different sizes of the central square cutout and boundary conditions.

Behavior of shell panel with eccentric cutout

Fundamental frequency

The effect of eccentricity of cutout positions on fundamental frequencies, are studied from the results obtained for different locations of a cutout with $a^/ /a$=0.2. The non-dimensional coordinates of the cutout centre ($\bar{x} = \frac{x}{a}, \bar{y} = \frac{y}{a}$) was varied from 0.2 to 0.8 along each directions, so that the distance of a cutout margin from the shell boundary was not less than one tenth of the plan dimension of the shell. The margins of cutouts were stiffened with four stiffeners. The study was carried out for all the thirteen boundary conditions for both cross ply and angle ply shells. The fundamental frequency of a shell with an eccentric cutout is expressed as a percentage of fundamental frequency of a shell with a concentric cutout. This percentage is denoted by r. In Tables 7 and 8 such results are furnished for a/b=1, a/h=100, $a^/ / b^/$ =1, c/a=0.2; E_{11}/E_{22} = 25, G_{23} = 0.2E_{22}, G_{13} = G_{12} = 0.5E_{22}, $\nu_{12} = \nu_{21}$ =0.25.

Table 7: Values of '*r*' for 0/90/0/90 hyperbolic paraboloid shells.

Edge condition	$\bar{y}$	$\bar{x}$						
		0.2	0.3	0.4	0.5	0.6	0.7	0.8
CCCC	0.2	82.88	86.09	92.60	99.80	92.60	86.10	82.88
	0.3	81.62	84.83	91.57	99.64	91.57	84.83	81.62
	0.4	83.23	86.19	92.48	99.75	92.48	86.19	83.23
	0.5	85.60	88.38	94.14	100	94.14	88.38	85.60
	0.6	83.23	86.19	92.48	99.85	92.48	86.19	83.23
	0.7	81.62	84.83	91.57	99.64	91.57	84.83	81.69
	0.8	82.62	85.82	92.31	99.78	92.52	85.88	82.72
CSCC	0.2	91.49	96.28	100.95	105.01	100.95	96.31	91.51
	0.3	91.46	96.97	104.34	110.17	104.36	97.00	91.46
	0.4	91.09	95.56	103.48	112.01	103.62	95.62	91.01
	0.5	88.02	89.69	94.66	100	94.97	89.83	87.79
	0.6	84.01	84.46	88.60	93.32	88.84	84.59	83.72
	0.7	82.15	82.44	86.47	90.93	86.64	82.54	81.88
	0.8	81.98	82.37	86.32	90.59	86.51	82.48	81.78
CCSC	0.2	73.72	77.82	85.97	100.54	106.08	94.91	87.48
	0.3	73.16	77.31	85.52	100.21	105.48	94.52	87.44
	0.4	73.36	77.32	85.32	99.77	105.38	94.06	86.47
	0.5	73.88	77.79	85.71	100	105.75	94.03	85.90
	0.6	73.36	77.32	85.32	99.77	105.38	94.06	86.47
	0.7	73.16	77.31	85.52	100.21	105.48	94.52	87.44
	0.8	73.49	77.59	85.71	100.50	105.99	94.68	87.29
CCCS	0.2	82.11	82.75	86.69	90.77	86.69	82.75	82.11
	0.3	82.17	82.77	86.77	91.09	86.77	82.77	82.17
	0.4	84.01	84.80	88.91	93.41	88.90	84.80	84.01
	0.5	88.12	90.05	94.98	100	94.98	90.05	88.11
	0.6	91.38	95.94	103.84	113.05	103.84	95.94	91.38
	0.7	91.82	97.37	104.78	110.54	104.78	97.37	91.82
	0.8	90.00	95.75	101.33	105.46	101.35	96.32	90.68
CSSC	0.2	71.77	79.96	91.50	107.07	107.29	93.76	82.91
	0.3	76.23	85.35	98.03	113.08	112.28	98.86	87.59
	0.4	75.40	82.61	93.92	112.04	116.08	101.45	89.19
	0.5	68.44	73.67	83.16	100	107.26	92.77	81.94
	0.6	62.08	66.80	76.05	93.07	99.39	85.43	75.41
	0.7	58.92	63.95	73.64	91.03	95.87	81.94	72.16
	0.8	58.21	63.64	73.59	91.04	94.92	80.97	71.21
CCSS	0.2	58.25	63.72	73.68	91.06	94.76	80.91	71.20
	0.3	58.90	63.97	73.65	91.02	95.64	81.83	72.12
	0.4	62.06	66.82	76.06	93.08	99.06	85.29	75.37
	0.5	68.42	73.69	83.16	100	106.87	92.61	81.89
	0.6	75.41	82.63	93.93	112.05	116.01	101.38	89.16
	0.7	76.25	85.36	98.05	113.10	112.30	98.88	87.60
	0.8	71.32	79.61	91.38	107.05	107.30	93.70	82.78

CSCS	0.2	82.39	82.75	86.02	89.24	86.02	82.75	82.39
	0.3	83.15	83.62	87.24	90.99	87.24	83.62	83.15
	0.4	85.43	86.25	90.30	94.62	90.30	86.25	85.43
	0.5	89.61	90.53	95.16	100	95.16	90.53	89.46
	0.6	85.43	86.25	90.29	94.62	90.30	86.25	85.43
	0.7	83.15	83.62	87.24	90.99	87.24	83.62	83.15
	0.8	82.33	82.71	85.99	89.25	86.01	82.76	82.38
SCSC	0.2	71.41	76.93	86.16	101.86	86.16	76.93	71.41
	0.3	71.56	76.94	86.05	100.83	86.04	76.94	71.56
	0.4	70.99	76.53	85.67	100.01	85.67	76.53	70.99
	0.5	70.69	76.48	85.81	100	85.81	76.48	70.69
	0.6	70.99	76.53	85.67	100.14	85.67	76.56	70.99
	0.7	71.56	76.94	86.05	100.56	86.04	76.94	71.56
	0.8	71.19	76.70	85.90	100.67	86.09	76.77	71.29
CSSS	0.2	51.72	59.07	70.82	89.60	92.64	77.23	65.92
	0.3	54.74	61.40	72.46	90.93	95.30	80.27	69.26
	0.4	59.74	66.11	76.46	94.37	100.12	85.32	74.24
	0.5	65.28	73.99	82.80	100	107.08	91.45	79.13
	0.6	59.74	66.11	76.46	94.37	100.12	85.32	74.24
	0.7	54.74	61.40	72.46	90.93	95.30	80.26	69.26
	0.8	51.71	59.06	70.79	89.58	92.61	77.22	65.90
SSSC	0.2	68.33	77.85	90.13	102.99	90.13	77.85	68.33
	0.3	72.36	82.73	96.11	107.63	96.11	82.73	72.36
	0.4	69.89	78.93	91.63	109.01	91.63	78.92	69.89
	0.5	62.18	69.81	80.99	100	80.99	69.81	62.18
	0.6	56.27	63.36	74.19	90.79	74.2	63.36	56.27
	0.7	53.77	60.90	71.95	88.98	71.95	60.90	53.77
	0.8	53.46	60.75	71.94	89.13	71.98	60.77	53.50
SSCS	0.2	65.92	77.23	92.64	89.60	70.82	59.07	51.72
	0.3	69.26	80.26	95.30	90.93	72.46	61.40	54.74
	0.4	74.24	85.32	100.12	94.37	76.46	66.11	59.74
	0.5	79.13	91.45	107.08	100	82.80	73.99	65.28
	0.6	74.24	85.32	100.12	94.37	76.46	66.11	59.74
	0.7	69.25	80.26	95.30	90.93	72.46	61.40	54.73
	0.8	65.90	77.22	92.63	89.58	70.79	59.05	51.70
SSSS	0.2	48.35	58.19	71.73	90.91	71.73	58.19	48.35
	0.3	51.21	60.39	73.30	92.10	73.30	60.39	51.21
	0.4	56.14	64.92	77.21	95.34	77.21	64.91	56.14
	0.5	62.58	72.14	83.37	100	83.37	72.14	62.57
	0.6	56.14	64.91	77.21	95.33	77.21	64.91	56.14
	0.7	51.21	60.38	73.30	92.10	73.30	60.39	51.21
	0.8	48.34	58.18	71.69	92.03	71.71	58.16	48.34
CS	0.2	87.88	97.94	104.11	107.44	104.11	97.94	87.88
	0.3	88.96	95.74	101.44	104.94	101.42	95.74	88.94
	0.4	90.09	93.54	98.07	101.64	98.07	93.51	90.09
	0.5	90.55	92.51	96.53	100	96.52	92.51	90.53
	0.6	90.09	93.54	98.09	101.64	98.07	93.54	90.09
	0.7	88.94	95.74	101.42	104.94	101.42	95.74	88.94
	0.8	87.81	97.72	103.79	107.37	103.84	97.72	87.83

Table 8: Values of '*r*' for +45/-45/+45/-45 hyperbolic paraboloid shells.

Edge condition	$\bar{y}$	$\bar{x}$						
		0.2	0.3	0.4	0.5	0.6	0.7	0.8
CCCC	0.2	65.33	69.87	77.01	86.18	76.94	69.82	65.30
	0.3	68.42	73.41	81.02	89.94	80.91	73.34	68.38
	0.4	73.59	79.17	87.27	95.50	87.15	79.08	73.54
	0.5	80.82	86.29	93.83	99.99	93.83	86.30	80.82
	0.6	73.54	79.08	87.15	95.50	87.27	79.17	73.58
	0.7	68.38	73.34	80.91	89.95	81.02	73.41	68.42
	0.8	65.30	69.82	76.93	86.18	77.01	69.87	65.33
CSCC	0.2	68.16	73.25	81.05	90.98	80.86	73.14	68.11
	0.3	71.86	77.24	85.42	95.23	85.21	77.12	71.80
	0.4	77.25	83.43	92.15	100.74	91.89	83.28	77.158
	0.5	73.80	81.40	91.44	100	91.51	80.99	73.14
	0.6	67.85	74.51	83.86	93.67	83.01	74.27	67.50
	0.7	64.65	70.70	79.37	89.27	79.35	70.50	64.44
	0.8	63.14	68.73	76.84	86.65	76.79	68.54	62.96
CCSC	0.2	66.83	70.25	75.70	84.69	81.61	74.12	69.42
	0.3	69.50	73.43	79.50	89.00	85.70	77.71	72.51
	0.4	74.02	78.64	85.43	95.16	92.27	83.71	77.79
	0.5	79.35	85.01	91.52	100	99.77	92.15	85.30
	0.6	73.49	77.95	84.60	94.33	92.55	83.90	77.91
	0.7	69.02	72.80	78.68	88.04	85.93	77.85	72.60
	0.8	66.42	69.69	74.95	83.78	81.77	74.24	69.50
CCCS	0.2	62.89	68.42	76.65	86.68	76.96	68.84	63.25
	0.3	64.33	70.32	79.12	94.53	79.49	70.81	64.75
	0.4	67.33	74.01	83.55	93.64	83.99	74.63	67.95
	0.5	72.89	80.62	91.07	100	91.58	81.53	73.91
	0.6	77.26	83.41	92.03	100.88	92.29	83.56	77.38
	0.7	71.92	77.24	85.34	95.38	85.56	77.36	71.97
	0.8	68.21	73.25	80.99	91.09	81.16	73.36	68.26
CSSC	0.2	70.74	74.99	81.37	91.13	87.59	79.20	73.63
	0.3	74.11	78.70	85.59	95.80	92.22	83.45	77.51
	0.4	74.46	82.22	91.91	101.91	99.20	90.05	83.45
	0.5	69.20	76.62	87.32	100	98.33	86.96	77.50
	0.6	64.99	71.37	80.57	92.91	90.40	79.69	71.36
	0.7	62.67	68.23	76.47	88.23	85.58	75.63	68.27
	0.8	61.49	66.58	74.37	85.63	82.84	73.56	66.89
CCSS	0.2	61.59	66.54	74.25	85.53	83.24	74.26	67.84
	0.3	62.68	68.11	76.35	88.25	85.96	76.40	69.40
	0.4	64.90	71.18	80.40	92.98	90.77	80.55	72.79
	0.5	68.99	76.33	87.09	100	98.65	87.98	79.22
	0.6	74.54	82.21	91.17	101.11	99.67	90.40	83.69
	0.7	73.79	78.07	84.68	94.79	92.65	83.76	77.73
	0.8	69.78	73.91	80.17	89.99	87.97	79.50	73.84

CSCS	0.2	63.68	69.60	78.21	88.23	78.50	69.99	64.04
	0.3	65.52	71.78	80.89	91.10	81.26	72.28	65.96
	0.4	68.67	75.63	85.47	95.54	85.92	76.26	69.28
	0.5	73.12	81.73	92.91	100	92.91	81.73	73.41
	0.6	69.28	76.26	85.93	95.54	85.47	75.63	68.67
	0.7	65.96	72.28	81.26	91.10	80.89	71.78	65.52
	0.8	64.03	69.99	78.50	88.21	78.19	69.59	63.67
SCSC	0.2	68.49	72.01	77.63	85.85	76.85	71.44	68.07
	0.3	71.21	75.28	81.50	89.85	80.67	74.62	70.71
	0.4	75.78	80.56	87.54	95.55	86.70	79.88	75.23
	0.5	81.15	86.92	93.58	100	93.58	86.92	81.15
	0.6	75.23	79.88	86.70	95.55	87.54	80.57	75.78
	0.7	70.71	74.62	80.67	89.85	81.51	75.27	71.21
	0.8	68.07	71.44	76.85	85.85	77.62	72.01	68.49
CSSS	0.2	60.83	66.45	75.08	86.92	84.29	74.84	67.87
	0.3	62.69	68.44	77.35	89.77	87.21	77.24	69.87
	0.4	64.63	71.18	81.32	94.53	92.17	81.64	73.73
	0.5	66.22	73.75	86.32	100	98.45	87.71	77.97
	0.6	64.61	71.24	81.38	94.37	91.27	80.25	71.93
	0.7	62.24	68.23	77.26	89.64	86.45	76.05	68.40
	0.8	59.80	65.71	74.67	86.70	83.67	68.04	66.65
SSSC	0.2	72.56	77.15	83.76	92.20	82.30	75.80	71.28
	0.3	76.08	80.93	88.07	96.76	86.86	79.98	75.31
	0.4	75.75	84.47	94.51	101.97	93.41	84.10	75.00
	0.5	69.58	78.21	89.51	100	88.70	77.13	68.11
	0.6	65.07	72.73	82.60	93.54	81.81	71.60	63.43
	0.7	62.89	69.52	78.40	89.06	77.65	68.44	61.36
	0.8	61.94	67.85	76.23	86.47	75.46	66.86	60.70
SSCS	0.2	66.65	73.88	83.68	86.72	74.69	65.74	59.83
	0.3	68.40	76.05	86.45	89.64	77.26	68.23	62.24
	0.4	71.93	80.26	91.27	94.37	81.37	71.24	64.61
	0.5	77.97	87.71	98.45	100	86.32	73.75	66.22
	0.6	73.73	81.65	92.17	94.53	81.31	71.18	64.63
	0.7	69.89	77.24	87.23	89.77	77.35	68.44	62.69
	0.8	67.86	74.84	84.28	86.90	75.03	66.40	60.80
SSSS	0.2	57.38	66.48	77.43	88.99	77.61	66.75	57.63
	0.3	59.29	68.18	79.58	91.81	80.01	68.85	59.97
	0.4	62.77	71.98	83.89	96.20	84.43	72.80	63.84
	0.5	68.08	78.21	91.21	100	91.21	78.21	68.08
	0.6	63.84	72.81	84.43	96.20	83.90	71.98	62.77
	0.7	59.97	68.85	80.01	91.81	79.58	68.18	59.29
	0.8	57.63	66.74	77.61	88.98	77.38	66.46	57.37
CS	0.2	64.80	72.96	83.43	92.90	85.34	74.61	66.23
	0.3	66.53	74.248	84.50	95.15	86.34	76.11	68.49
	0.4	67.75	75.73	86.40	98.11	88.03	77.54	69.61
	0.5	68.95	77.16	88.29	100	88.29	77.16	68.95
	0.6	69.63	77.56	88.03	98.10	86.40	63.44	67.75
	0.7	68.51	76.13	86.34	95.17	84.52	74.25	66.53
	0.8	66.21	74.55	85.22	92.90	83.23	72.88	64.76

Table 9: Maximum values of *r* with corresponding coordinates of cutout centres and zones where $r \geq 90$ and $r \geq 95$ for 0/90/0/90 hyperbolic paraboloid shells

Boundary Condition	Maximum values of r	Co-ordinate of cutout centre	Area in which the value of r≥90	Area in which the value r≥95
CCCC	100.00	(0.5,0.5)	$\bar{x}$=0.4, 0.6 $0.2 \leq \bar{y} \leq 0.8$	$\bar{x}$=0.5 $0.2 \leq \bar{y} \leq 0.8$
CSCC	105.01	(0.5,0.2)	$\bar{x}$=0.2,0.8 $0.2 \leq \bar{y} \leq 0.4$; $\bar{x}$=0.5, $0.5 \leq \bar{y} \leq 0.8$	$0.3 \leq \bar{x} \leq 0.7$ $0.2 \leq \bar{y} \leq 0.4$
CCSC	106.08	(0.6,0.2)	$\bar{x}$=0.7, $0.2 \leq \bar{y} \leq 0.8$	$0.5 \leq \bar{x} \leq 0.6$ $0.2 \leq \bar{y} \leq 0.8$
CCCS	113.05	(0.5,0.6)	$\bar{x}$=0.2,0.8, $0.6 \leq \bar{y} \leq 0.8$; $0.3 \leq \bar{x} \leq 0.7$, $\bar{y}$=0.5	$0.3 \leq \bar{x} \leq 0.7$ $0.6 \leq \bar{y} \leq 0.8$
CSSC	116.08	(0.6,0.4)	Nil	$0.5 \leq \bar{x} \leq 0.6$ $0.2 \leq \bar{y} \leq 0.5$
CCSS	116.01	(0.6,0.6)	Nil	$0.5 \leq \bar{x} \leq 0.6$ $0.5 \leq \bar{y} \leq 0.8$
CSCS	100.00	(0.5,0.5)	$0.4 \leq \bar{x} \leq 0.6$, $0.4 \leq \bar{y} \leq 0.6$	$0.4 \leq \bar{x} \leq 0.6$ $\bar{y}$=0.5
SCSC	101.86	(0.5,0.2)	Nil	$\bar{x}$=0.5 $0.2 \leq \bar{y} \leq 0.8$
CSSS	107.08	(0.6,0.5)	$\bar{x}$=0.5 $0.3 \leq \bar{y} \leq 0.7$	$\bar{x}$=0.6 $0.3 \leq \bar{y} \leq 0.7$
SSSC	109.01	(0.5,0.4)	$\bar{x}$=0.4, 0.6 $0.2 \leq \bar{y} \leq 0.4$	$\bar{x}$=0.5 $0.2 \leq \bar{y} \leq 0.5$
SSCS	107.08	(0.4,0.5)	$\bar{x}$=0.5 $0.3 \leq \bar{y} \leq 0.7$	$\bar{x}$=0.4 $0.3 \leq \bar{y} \leq 0.7$
SSSS	100.00	(0.5,0.5)	$\bar{x}$=0.5,$0.2 \leq \bar{y} \leq 0.8$	$\bar{x}$=0.5, $\bar{y}$=0.5
CS	107.37	(0.5,0.8)	The whole area except corner points.	$0.4 \leq \bar{x} \leq 0.6$ $0.2 \leq \bar{y} \leq 0.8$

$a/b=1$, $a/h=100$, $a'/b'=1$, $c/a=0.2$; $E_{11}/E_{22}=25$, $G_{23}=0.2E_{22}$, $G_{13}=G_{12}=0.5E_{22}$, $\nu_{12}=\nu_{21}=0.25$.

It can be seen that eccentricity of the cutout along the length of the shell towards the clamped edges makes it more flexible. It is also seen that almost all the cases r value is maximum in and around $\bar{x}=0.5$ and $\bar{y}=0.5$. When edge, opposite to a clamped edge is simply supported, r value first increases towards the simply supported edge then decreases. But, when two opposite edges are simply supported r value decreases towards the simply supported edges. Again in case of an angle ply shell, if the simply supported edge be the hyperbolic one then r value decreases towards the edge. So, for functional purposes, if a shift of central cutout is required, eccentricity of a cutout along the length or width should preferably be towards the simply supported edge which is opposite to a clamped edge for cross ply shells. For angle ply shells eccentricity towards simply supported hyperbolic edge should be avoided.

Table 10: Maximum values of *r* with corresponding coordinates of cutout centres and zones where $r \geq 90$ and $r \geq 95$ for +45/-45/+45/-45 hyperbolic paraboloid shells

Boundary Condition	Maximum values of r	Co-ordinate of cutout centre	Area in which the value of r≥90	Area in which the value r≥95
CCCC	100.00	(0.5,0.5)	$0.4 \leq \bar{x} \leq 0.6$, $\bar{y}=0.5$	$\bar{x}=0.5$, $0.4 \leq \bar{y} \leq 0.6$
CSCC	100.74	(0.5,0.4)	No rectangular zone but some discrete points around centre	$\bar{x}=0.5$, $0.3 \leq \bar{y} \leq 0.5$
CCSC	100.00	(0.5,0.5)	No rectangular zone but some discrete points around centre	$\bar{x}=0.5$, $\bar{y}=0.4, 0.5$; $\bar{x}=0.6$, $\bar{y}=0.5$
CCCS	100.89	(0.5,0.6)	No rectangular zone but some discrete points around centre	$\bar{x}=0.5$, $0.5 \leq \bar{y} \leq 0.7$
CSSC	101.91	(0.5,0.4)	No rectangular zone but some discrete points around centre	$\bar{x}=0.5$, $0.3 \leq \bar{y} \leq 0.5$; $\bar{x}=0.6$, $0.4 \leq \bar{y} \leq 0.5$
CCSS	101.11	(0.5,0.6)	No rectangular zone but some discrete points around centre	$0.5 \leq \bar{x} \leq 0.6$, $0.5 \leq \bar{y} \leq 0.6$
CSCS	100.00	(0.5,0.5)	No rectangular zone but some discrete points around centre	$\bar{x}=0.5$, $0.4 \leq \bar{y} \leq 0.6$
SCSC	100.00	(0.5,0.5)	No rectangular zone but some discrete points around centre	$\bar{x}=0.5$, $0.4 \leq \bar{y} \leq 0.6$
CSSS	100.00	(0.5,0.5)	No rectangular zone but some discrete points around centre	$\bar{x}=0.5, 0.6$ $\bar{y}=0.5$
SSSC	101.97	(0.5,0.4)	No rectangular zone but some discrete points around centre	$\bar{x}=0.5$, $0.3 \leq \bar{y} \leq 0.5$
SSCS	100.00	(0.5,0.5)	No rectangular zone but some discrete points around centre	$\bar{x}=0.4,0.5$ $\bar{y}=0.5$
SSSS	100.00	(0.5,0.5)	No rectangular zone but some discrete points around centre	$\bar{x}=0.5$, $0.4 \leq \bar{y} \leq 0.6$
CS	100.00	(0.5,0.5)	No rectangular zone but some discrete points around centre	$\bar{x}=0.5$, $0.3 \leq \bar{y} \leq 0.7$

$a/b=1$, $a/h=100$, $a'/b'=1$, $c/a=0.2$; $E_{11}/E_{22}=25$, $G_{23}=0.2E_{22}$, $G_{13}=G_{12}=0.5E_{22}$, $\nu_{12}=\nu_{21}=0.25$.

Tables 9 and 10 provide the maximum values of r together with the position of the cutout. These tables also show the rectangular zones within which r is always greater than or equal to 90 and 95. It is to be noted that at some other points r values may have similar values, but only the zone rectangular in plan has been identified. These tables indicate the maximum eccentricity of a cutout which can be permitted if the fundamental frequency of a concentrically punctured shell is not to reduce a drastic amount. So these tables will help practicing engineers.

Mode shapes

The mode shapes corresponding to the fundamental modes of vibration are plotted in Figs.4-11 for cross-ply and angle ply shell of CCCC CCSC, SCSC and SSSC boundary conditions for different eccentric position of the cutout. All the mode shapes are either bending or torsion mode. It is found that for different position of cutout mode shapes are somewhat similar to one another, only the crest and trough position changes.

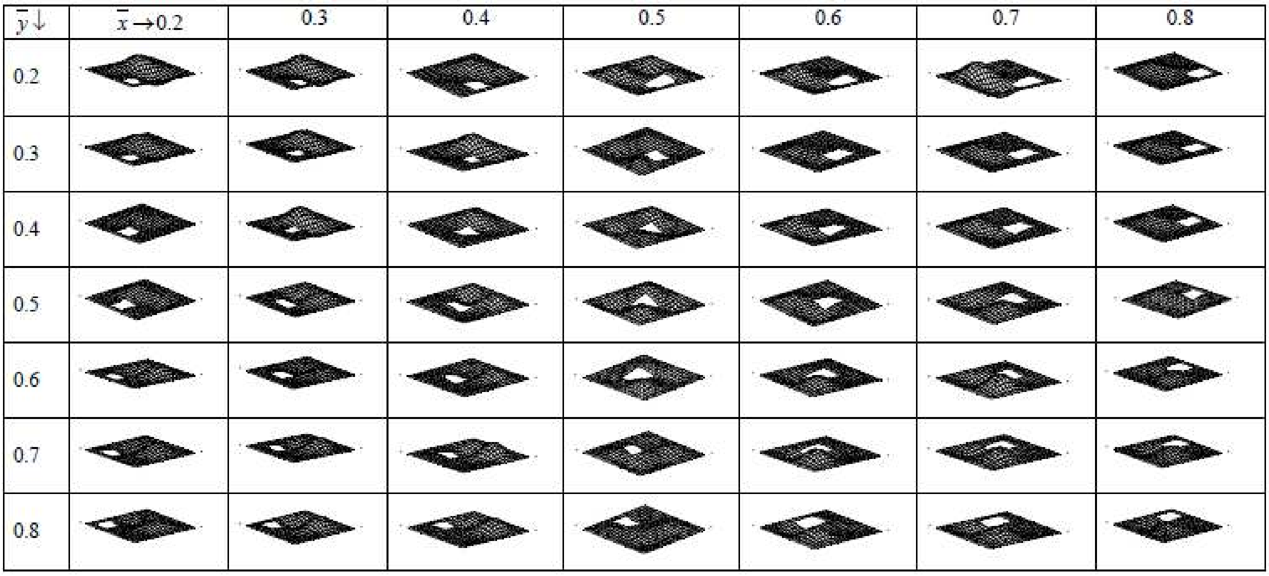

Fig.4: First mode shapes of laminated composite (0/90/0/90) stiffened rectangular hyperbolic paraboloidal shell for different position of the central square cutout and CCCC boundary condition.

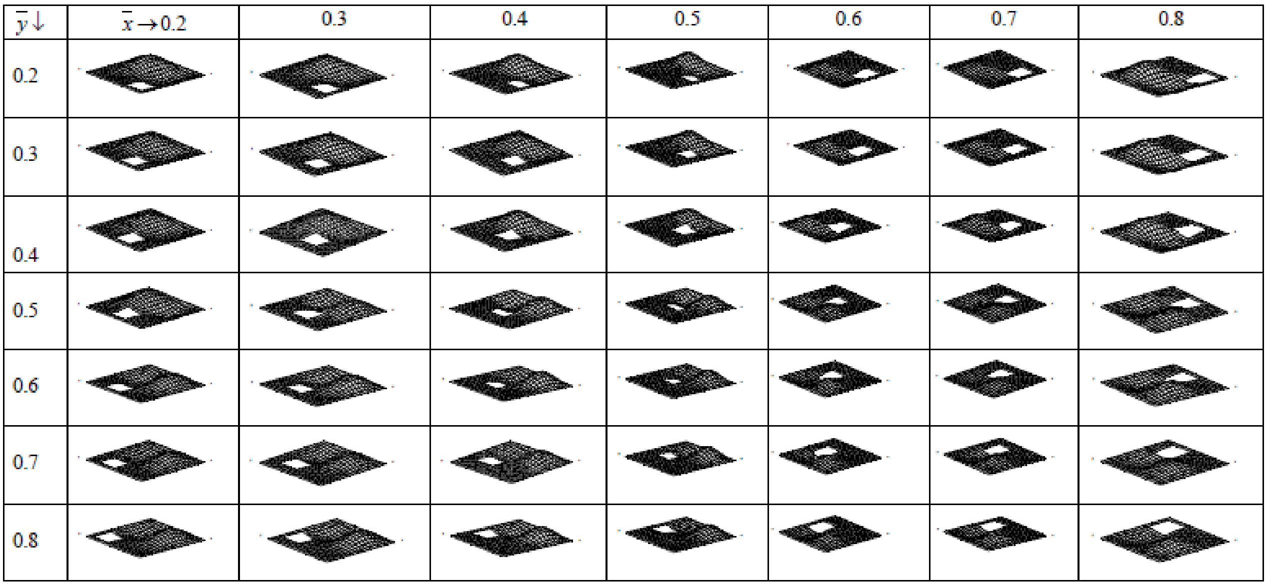

Fig.5: First mode shapes of laminated composite (0/90/0/90) stiffened rectangular hyperbolic paraboloidal shell for different position of the central square cutout and CCSC boundary condition.

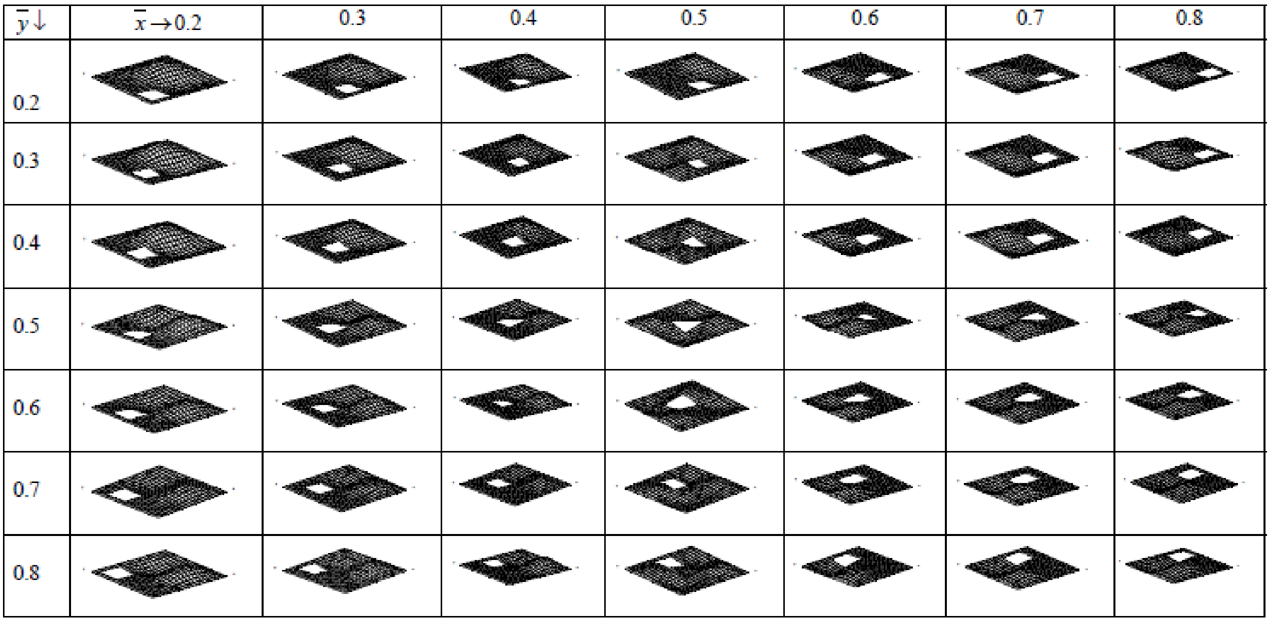

Fig.6: First mode shapes of laminated composite (0/90/0/90) stiffened rectangular hyperbolic paraboloidal shell for different position of the central square cutout and SCSC boundary condition.

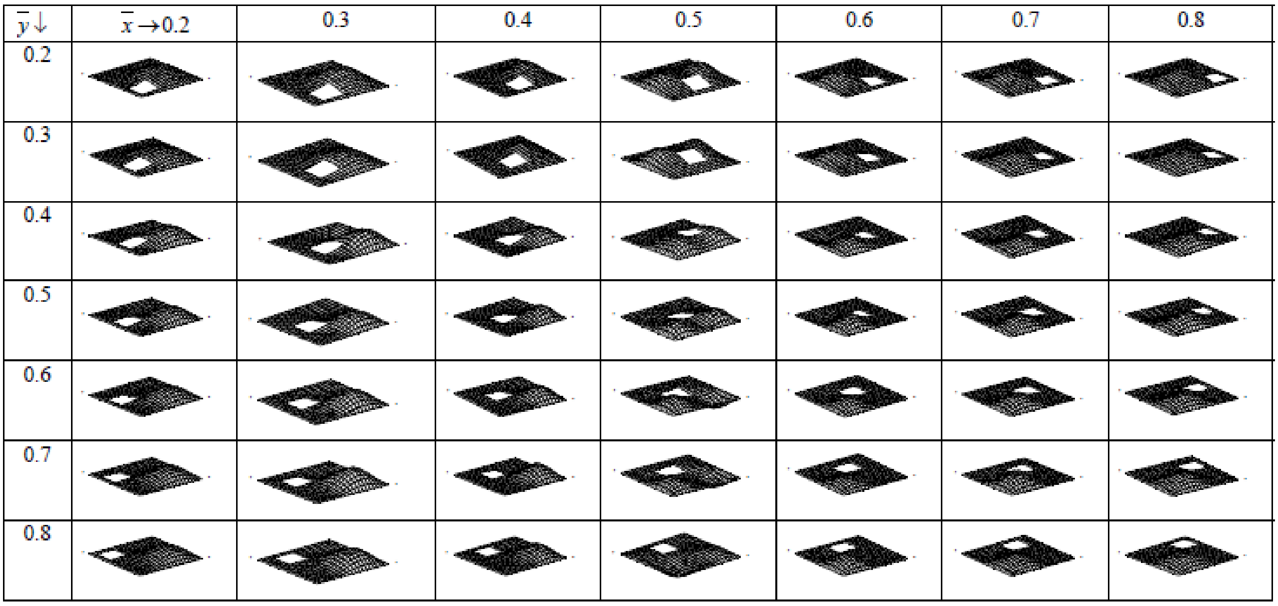

Fig.7: First mode shapes of laminated composite (0/90/0/90) stiffened rectangular hyperbolic paraboloidal shell for different position of the central square cutout and SSSC boundary condition.

CONCLUSIONS

The finite element code used here is suitable for analyzing free vibration problems of stiffened hyperbolic paraboloid shell panels with cutouts, as this approach produces results in close agreement with those of the benchmark problems. Free vibration characteristics mostly depend on the arrangement of boundary constraints along the four edges rather than their actual number. If two edges are released for any functional reason, then two alternate edges must release instead of two adjacent edges. The relative free vibration performances of shells for different combinations of edge conditions along the four sides are expected to be very helpful in decision-making for practicing

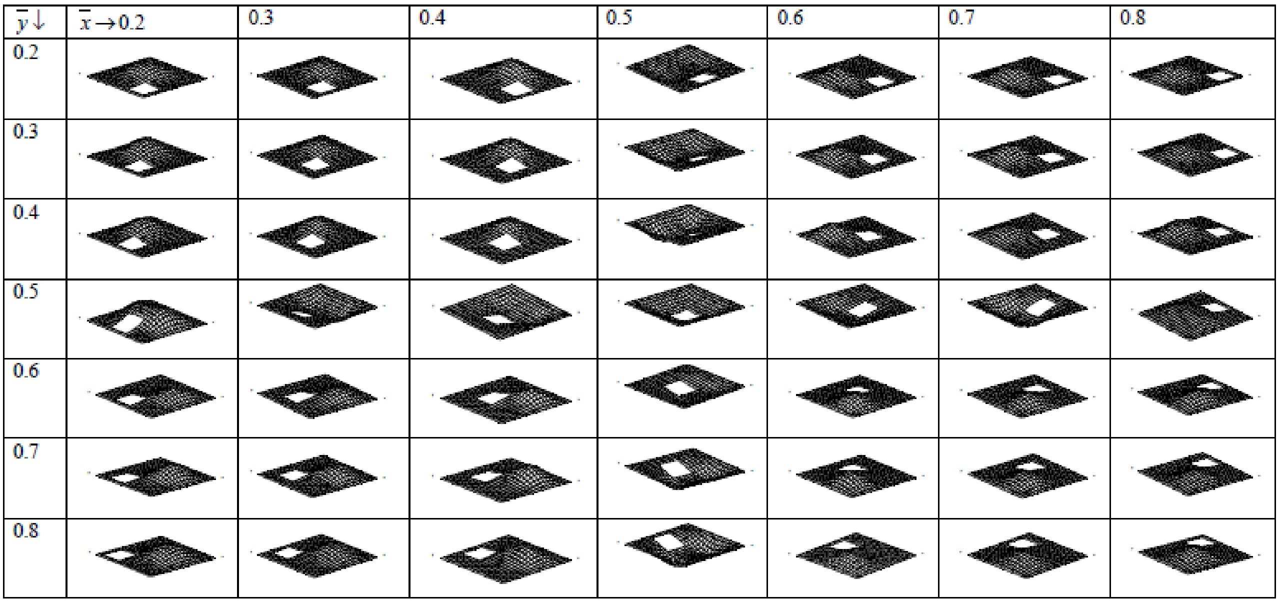

Fig.8: First mode shapes of laminated composite (+45/-45/+45/-45) stiffened rectangular hyperbolic paraboloidal shell for different position of the central square cutout and CCCC boundary condition.

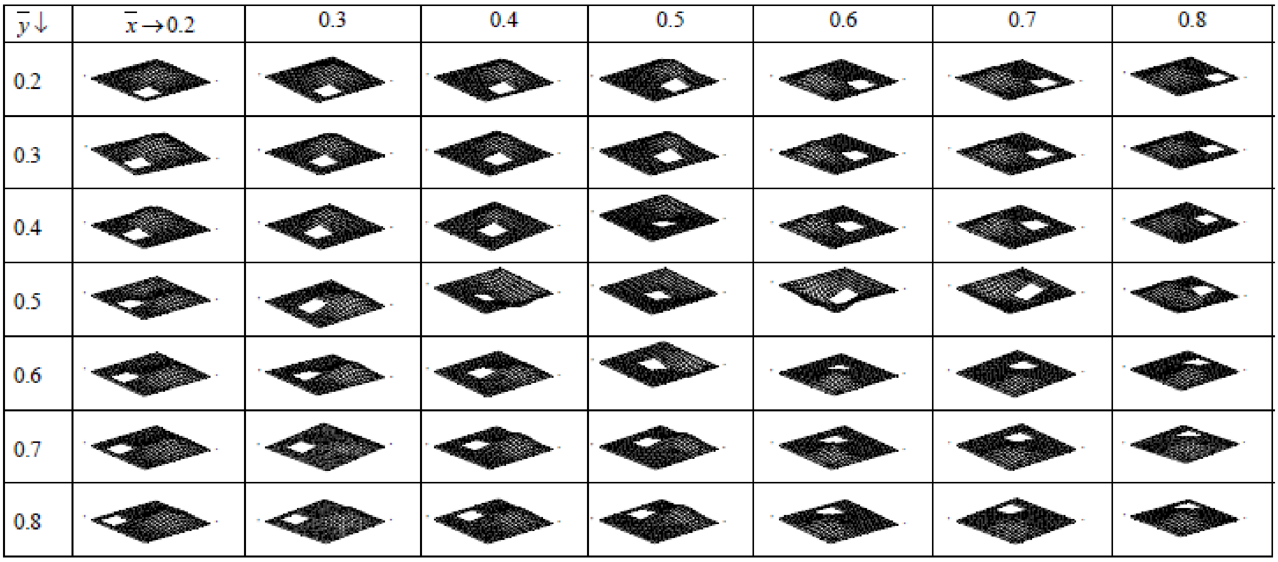

Fig.9: First mode shapes of laminated composite (+45/-45/+45/-45) stiffened rectangular hyperbolic paraboloidal shell for different position of the central square cutout and CCSC boundary condition.

engineers. For functional purposes, if a shift of central cutout is required, eccentricity of a cutout along the length or width should preferably be towards the simply supported edge which is opposite to a clamped edge for cross ply shells. For angle ply shells eccentricity towards simply supported hyperbolic edge should be avoided. The information regarding the behaviour of stiffened hyperbolic paraboloid shell with eccentric cutouts for a wide spectrum of eccentricity and boundary conditions for cross ply and angle ply shells may also be used as design aids for structural engineers. The present study provides the specific zones within which the cutout centre may be moved so that the loss of frequency is less than 5% and 10% with respect to a shell with a central cutout. That will help an engineer to make a decision regarding the eccentricity of the cutout centre that can be allowed.

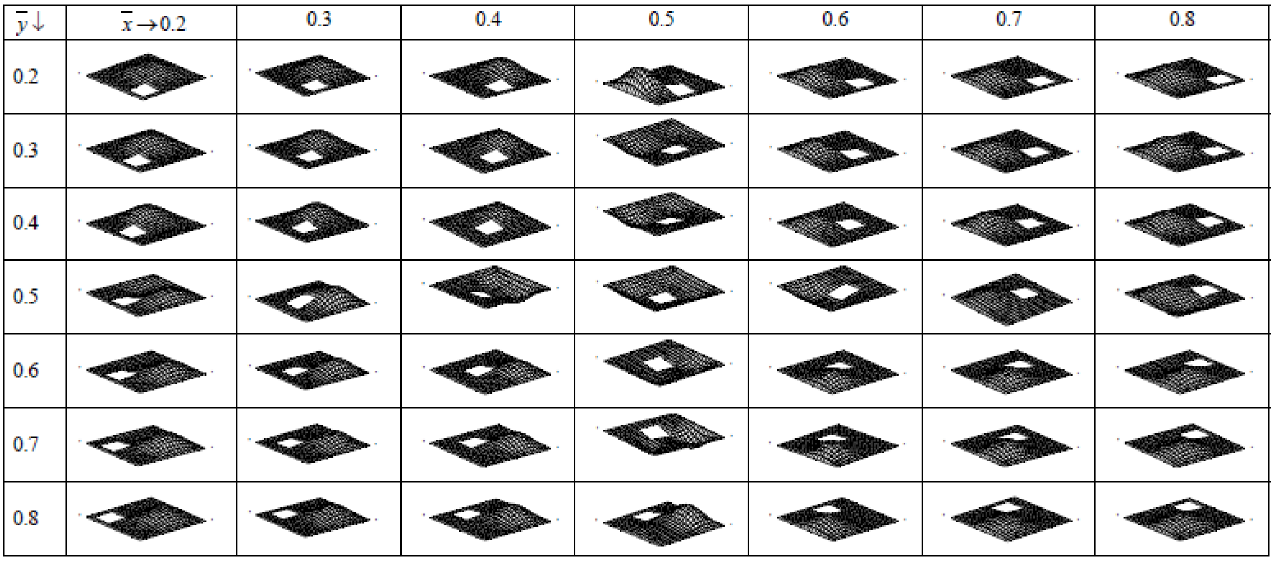

Fig.10: First mode shapes of laminated composite (+45/-45/+45/-45) stiffened rectangular hyperbolic paraboloidal shell for different position of the central square cutout and SCSC boundary condition.

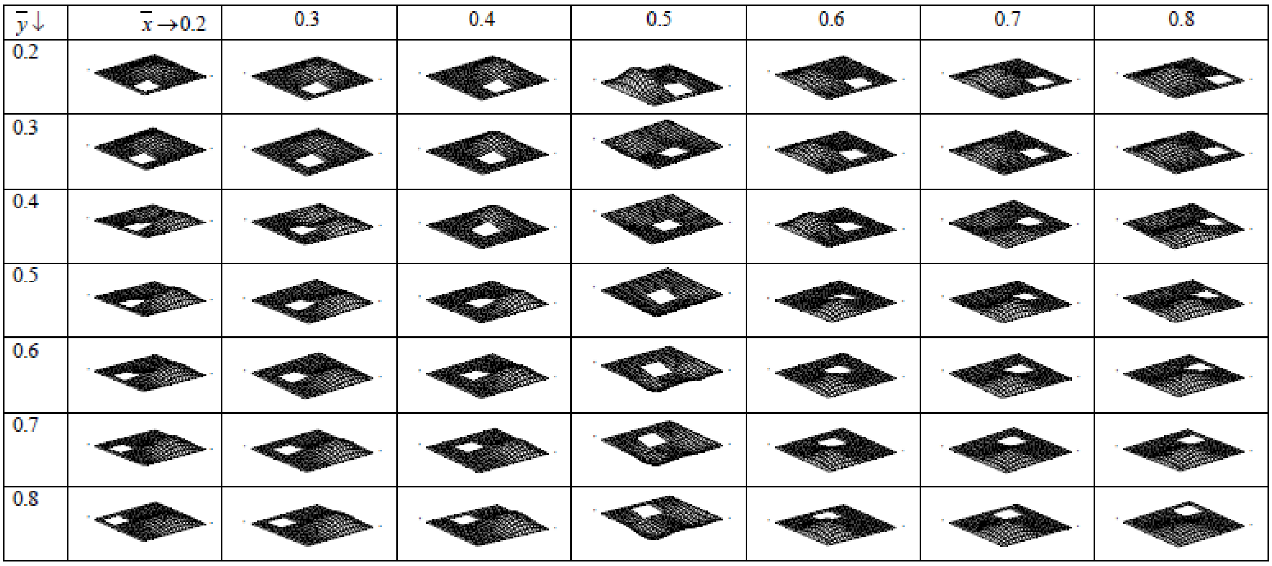

Fig.11: First mode shapes of laminated composite (+45/-45/+45/-45) stiffened rectangular hyperbolic paraboloidal shell for different position of the central square cutout and SSSC boundary condition.

REFERENCES

[1] B. Ghosh, J.N. Bandyopadhyay, Analysis of paraboloid of revolution type shell structures using isoparametric doubly curved shell elements, Computers & Structures, 36(5) (1990) 791-800.

[2] A. Dey, J.N. Bandyopadhyay, P.K. Sinha, Finite element analysis of laminated composite paraboloid of revolution shells, Computers & Structures, 44(3) (1992) 675-682.

[3] A. Dey, J.N. Bandyopadhyay, P.K. Sinha, Technical note: Behaviour of paraboloid of revolution shell using cross-ply and anti-symmetric angle-ply laminates, Computers & Structures, 52(6) (1994) 1301-1308.

[4] D. Chakravorty, P.K. Sinha, J.N. Bandyopadhyay, Free vibration analysis of point supported laminated composite doubly curved shells- a finite element approach, Computers & Structures, 54(2) (1995) 191-207.

[5] D. Chakravorty, P.K. Sinha, J.N. Bandyopadhyay, Finite element free vibration analysis of doubly curved laminated composite shells, J. Sound and Vibration, 191(4) (1996) 491-504.
[6] A.N. Nayak, J.N. Bandyopadhyay, Free vibration analysis and design aids of stiffened conoidal shells. Journal of Engineering Mechanics, 128 (2002) 419-427.
[7] A.N. Nayak, J.N. Bandyopadhyay, Free vibration analysis of laminated stiffened shells. Journal of Engineering Mechanics, 131 (2005) 100-105.
[8] A.N. Nayak, J.N. Bandyopadhyay, Dynamic response analysis of stiffened conoidal shells, Journal of Sound and Vibration, 291 (2006) 1288-1297.
[9] H.S. Das, D. Chakravorty, Design aids and selection guidelines for composite conoidal shell roofs-a finite element application, Journal of Reinforced Plastic and Composites, 26 (2007) 1793-1819.
[10] H.S. Das, D. Chakravorty, Natural frequencies and mode shapes of composite conoids with complicated boundary conditions, Journal of Reinforced Plastic and Composites, 27 (2008) 1397-1415.
[11] H.S. Das, D. Chakravorty, Finite element application in analysis and design of point supported composite conoidal shell roofs suggesting selection guidelines, Journal of Strain Analysis in Engineering Design., 45(3) (2010) 165-177.
[12] H.S. Das, D. Chakravorty, Bending analysis of stiffened composite conoidal shell roofs through finite element application. Journal of Composite Materials, 45 (2011) 525-542.
[13] S. Pradyumna, J.N. Bandyopadhyay, Static and free vibration analyses of laminated shells using a higher order theory. Journal of Reinforced Plastics and Composites, 27 (2008) 167-186.
[14] S. Pradyumna, J.N. Bandyopadhyay, Dynamic instability behaviour of laminated hypar and conoid shells using a higher-order shear deformation theory, Thin Walled Structures, 49 (2011) 77-84.
[15] J.N. Reddy, Large amplitude flexural vibration of layered composite plates with cutouts, Journal of Sound and Vibration, 83(1) (1982) 1-10.
[16] S.K. Malhotra, N. Ganesan, M.A. Veluswami, Vibration of composite plate with cutouts, Journal of Aeronautical Society of India, 41 (1989) 61-64.
[17] B. Sivasubramanian, A.M. Kulkarni, G.V. Rao, A. Krishnan, Free vibration of curved panels with cutouts, Journal of Sound and Vibration, 200(2) (1997) 227-234.
[18] K. Sivakumar, N.G.R. Iyengar, K. Deb, Free vibration of laminated composite plates with cutout, Journal of sound and Vibration, 221(3) (1999) 443-465.
[19] R.E. Rossi, Transverse vibrations of thin, orthotropic rectangular plates with rectangular cutouts with fixed boundaries, Journal of Sound and Vibration, 221(4) (1999) 733-736.
[20] M. Huang, T. Sakiyama, Free vibration analysis of rectangular plates with variously-shaped holes, Journal of Sound and Vibration, 226(4) (1999) 769-786.
[21] S.S. Hota, P. Padhi, Vibration of plates with arbitrary shapes of cutouts, Journal of Sound and Vibration, 302(4-5) (2007) 1030-1036.
[22] D. Chakravorty, P.K. Sinha, J.N. Bandyopadhyay, Applications of FEM on free and forced vibration of laminated shells, Journal of Engineering Mechanics; 124(1) (1998) 1-8.
[23] B. Sivasubramonian, G.V. Rao, A. Krishnan, Free vibration of longitudinally stiffened curved panels with cutout, Journal of Sound and Vibration, 226(1) (1999) 41-55.
[24] S.S. Hota, D. Chakravorty, Free vibration of stiffened conoidal shell roofs with cutouts, Journal of Vibration and Control, 13(3) (2007) 221-240.
[25] N. Nanda, J.N. Bandyopadhyay, Nonlinear free vibration analysis of laminated composite cylindrical shells with cutouts, Journal of Reinforced Plastic and Composites, 26(14) (2007) 143-1427.
[26] A. Kumar, A. Chakrabarti, P. Bhargava, Vibration of composite cylindrical shells with cutouts using higher order theory, International Journal of Scientific and Industrial Research, 5(4) (2013) 199-202.

[27] V.V. Vasiliev, R.M. Jones, L.L. Man, *Mechanics of Composite Structures,* Taylor and Francis, USA, (1993).
[28] M S. Qatu, *Vibration of Laminated Shells and Plates*, Elsevier, UK, (2004).
[29] S. Sahoo, D. Chakravorty, Finite element bending behaviour of composite hyperbolic paraboloid shells with various edge conditions, Journal of Strain Analysis for Engineering Design, 39(5) (2004) 499-513.
[31] A. Mukherjee, M. Mukhopadhyay, Finite element free vibration of eccentrically stiffened plates, Computers and Structures, 30 (1998) 1303-1317.
[32] A.N. Nayak, J.N. Bandyopadhyay, On the free vibration of stiffened shallow shells, Journal of Sound and Vibration, 255(2) (2002) 357-382.